Eur. Phys. J. Plus (2023) 138:384
https://doi.org/10.1140/epjp/s13360-023-03991-6

THE EUROPEAN PHYSICAL JOURNAL PLUS

Regular Article

Towards the development of a polymer-based assembly for cryogenic detectors for neutrino-less double beta decay

Matteo Biassoni[1,a], **Chiara Brofferio**[1,2], **Marco Faverzani**[1,2], **Elena Ferri**[1], **Irene Nutini**[1], **Valerio Pettinacci**[3], **Stefano Pozzi**[1,2], **Stefano Ghislandi**[4,5], **Simone Quitadamo**[4,5]

[1] *Present Address:* Istituto Nazionale di Fisica Nucleare, Sezione di Milano-Bicocca, Milan, Italy
[2] University of Milano-Bicocca, Milan, Italy
[3] Istituto Nazionale di Fisica Nucleare, Sezione di Roma1, Rome, Italy
[4] Gran Sasso Science Institute, L'Aquila, Italy
[5] Istituto Nazionale di Fisica Nucleare, GSGC, L'Aquila, Italy

Received: 18 November 2022 / Accepted: 10 April 2023

Abstract Cryogenic single-particle detectors are devices, operated close to absolute zero, widely used in current and future generation detectors for the search for rare particle physics processes, for example neutrino-less double beta decay. Traditionally, these detectors are assembled in copper structures inside dilution refrigerators. The use of copper, however, is expected to become a limiting factor on the path towards the background reduction needed for future generation projects. Its high density and large Z make it an effective target where gamma-rays produced by radioactive contaminants can lose part of their energy undetected, and subsequently be measured as sensitivity-spoiling spurious signals in the region of interest of the energy spectrum. We present here a new method of building assemblies for kg-scale cryogenic single particle detectors based on low Z, low density additive manufacturing-compatible polymers that can in the future be doped with scintillating compounds thus making them an active component of the experimental setup. Additive manufacturing overcomes the limitations, imposed by traditional techniques, in the design of the structures. The assembly geometry can therefore be driven by the combined needs for reduction of mass and optimization of light production and collection. The experimental setup and the performance of the detectors in terms of energy resolution and temperature stability are described.

1 Search for neutrino-less double beta decay

Within the particle physics and astroparticle community the interest in neutrino physics has been constantly growing since its discovery. Its phenomenology, related to the presence of its small but non-vanishing mass, is today the main tangible proof that a theory beyond the Standard Model is needed to fully describe the fundamental properties of nature [1]. The search for neutrino-less double beta decay (NDBD), in particular, is considered of paramount importance [2]: the observation of this lepton number-violating nuclear decay would be the proof that lepton number is not a conserved quantity (which means that matter-creating processes exist in nature) and neutrinos are Majorana fermions, i.e. they coincide with their own antiparticles. The discovery of this process could justify, among other things, the currently unexplained asymmetry of matter and antimatter in our universe. NDBD is an alternative and much rarer decay channel to the ordinary two-neutrino double beta-decay, where two neutrons in a (typically) heavy nucleus simultaneously undergo beta decay, changing the atomic number of the decaying element by two units but no neutrinos are emitted. The measured half-lives of double beta decaying nuclei are in the 10^{19}–10^{24} yr range, already making two-neutrino double beta decay a very rare process. In order to be sensitive to the even rarer neutrino-less version of the process, on the probability of which only limits corresponding to half-lives above 10^{25} years exist for most nuclei [3–8], extremely performing detectors are required, with an excellent energy resolution of few keV at the transition Q-value, large mass (ton to multi-ton scale) and almost no residual background potentially polluting the energy spectrum after passive shielding, material selection and active rejection [9–17].

2 State of the art: cryogenic single-particle detectors for rare events

A variety of detector technologies have been applied to the search for rare events in general [18–20], and NDBD in particular, and cryogenic detectors are one of the most promising. A kg-scale energy absorber, made of an inorganic crystal, containing the isotope

Focus Point on Advances in Cryogenic Detectors for Dark Matter, Neutrino Physics and Astrophysics Guest editor: L. Pattavina.

[a] e-mail: matteo.biassoni@mib.infn.it (corresponding author)

Published online: 05 May 2023

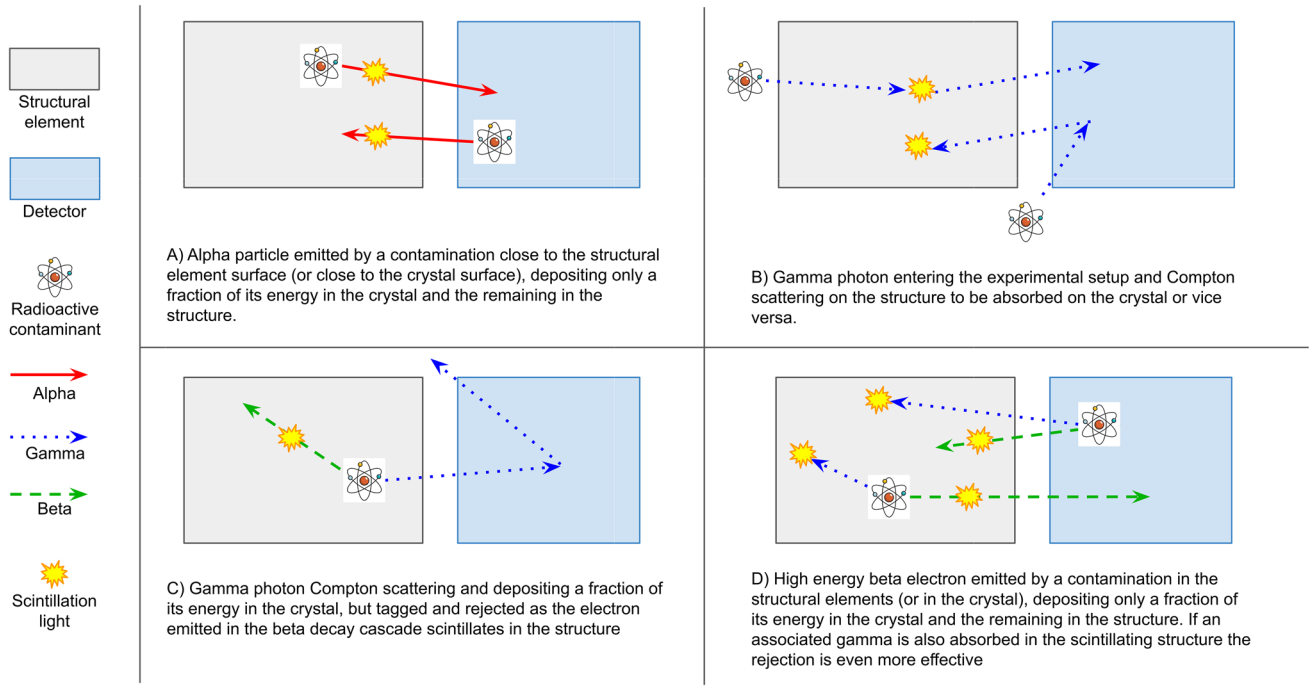

Fig. 1 Topology of background events involving the mechanical structure of the detector. All these types of events can be suppressed with a light and active structure

under study, is stably kept at temperatures very close to the absolute zero (typically ∼10 mK), where its thermal capacity is so low that even small energy depositions induce a sizeable temperature variation, measured precisely by a thermometer coupled to the absorber. The energy resolution [13, 21, 22] is comparable to that of semiconductor detectors for alpha and gamma spectroscopy, while the absence of any dead layer and the coincidence of the source with the absorber guarantee a high detection efficiency. Cryogenic detectors are typically mounted into structures made of high thermal conductivity materials, such as copper [23–26]; these structures act both as mechanical support and as a thermal link to the cryostat, providing the cooling power required to keep the active elements at the working temperature.

2.1 Background contribution from mechanical structure

The passive nature, high density and high Z of the described supporting structures, however, is expected to introduce a relevant contribution to the background of future experiments [27, 28]. Radiation generated by contaminants, both inside the structure or in its surroundings, can indeed lose part of its energy in a passive element of the setup and later be absorbed by the crystals, possibly becoming an irreducible background in the region of interest (ROI). These effects and background sources are routinely studied by current generation experiments [3, 5, 28–31]. Figure 1 shows a schematic depiction of the most relevant topologies of this kind of events. In all cases only part of the original particle energy is deposited in the active element (detector), and the remaining energy is either lost or absorbed in the surrounding structural elements. The possibility of replacing heavy passive materials with light and possibly scintillating ones (coupled with photo-sensors for the scintillation readout) for the construction of these structural elements is the focus of this work.

We describe in this paper the current status of the R &D on this approach, where the passive copper elements of the supporting structure are replaced with low-Z, low-density plastic materials (in particular acrylic). Acrylic can be produced with very high radio-purity (of the order of few μBq/kg of U and Th, comparable with the typical contamination of the copper used by the CUORE experiment for the detector structure [30]), as demonstrated by its use, for example for the vessel of the SNO experiment [32]. If needed, these materials could be made active by doping with scintillating compounds [33] and can be combined with additive manufacturing [34]. The readout of scintillation light is not the focus of this paper and has not been tested in the described measurement. The details of its implementation are strongly dependent on the specific experimental setup but both high-performance cryogenic light detectors [35–37] or collection and transport of the light to a SiPM readout with wavelength shifting fibres [38] are considered viable and demonstrated options. Additive manufacturing—implementing photo-sensitive resins—represents a frontier technology for the realization of thermal detector structures as it overcomes the limitations, imposed by traditional techniques, in the design of the structures. The choice of the assembly geometry can therefore be driven by the combined needs for the reduction of mass and optimization of light production and collection (whenever scintillation is implemented in the material).

2.2 Application scenarios

Probably, the most natural and direct application of the technique described in this paper are to the future of the search for double beta decay with thermal detectors [39, 40]. In order to compete with the other techniques, the next generation of cryogenic experiments is required to lower the background level in the ROI by one to two orders of magnitude with respect to the current generation, while the improvement for the future generations will have to be even higher [39, 41]. The largest representative of the current generation is the CUORE experiment, which is collecting science data and studying in great detail the contributions to its background in the ROI [3]. The main contribution (∼90%) at this stage are the degraded alpha particles emitted by contaminants on (or close to) the surface of passive structural elements (copper) facing the active crystals. This contribution can be strongly suppressed with the double-readout technique demonstrated by smaller (but still comparably sensitive) scale experiments like CUPID-0 [11] and CUPID-Mo [12]. In this case the heat signal is combined with the scintillation light emitted by the crystal itself (and recorded by a second dedicated thermal light-detector) to distinguish alpha from beta particles based on the relative quenching factor. This technology, which is foreseen to be used by the CUPID [27] and AMoRE [42] experiments with ^{100}Mo for the first time in a ton-scale project, although very effective, has the drawback of limiting the choice of the isotope to be studied to those that can be included in a scintillating crystal with good light yield and optical properties, de-facto reducing the potentiality for multi-isotope studies [43, 44]. Tellurium, for example, although being a very convenient choice for the CUORE experiment, despite numerous efforts cannot be used to grow crystals that scintillate at the required level [45]. A structure like the one proposed in this work, that can be made active via scintillation, would mitigate or eliminate the alpha background also in experiments based on non-scintillating crystals. A somewhat similar idea has been explored by the ABSuRD R &D [46] with a less radical approach where a scintillating coating is applied to the surface of traditional copper structures. Moreover, the alpha discrimination capabilities resulting from the use of a scintillating crystal and an active supporting structure are not mutually exclusive (as demonstrated by the CRESST experiment for the search for dark matter [47]), and could potentially be combined in future projects. Once the alpha background has been reduced by implementing particle identification (and other contributions, like pile-up between two-neutrino double beta decay events [48] and un-tagged cosmic muons, have been independently addressed), the remaining background is dominated by gamma and beta events from naturally occurring radioactive chains. This contribution is effectively reduced by selecting an isotope with a Q-value above the 2615 keV gamma line from natural radioactivity (^{100}Mo for CUPID and AMoRE as opposed to ^{130}Te used by CUORE, for example). This approach, however, is tactical in nature and it effectively reduces the number of isotopes that can be studied. Much more rare gamma transitions, moreover, exist in the natural radioactive chains and will inevitably start to play an important role as the sensitivity of the projects increases and the required level of background decreases. The impact of gamma radiation coming from far sources and surviving the shielding layers needs to be mitigated by removing any passive material in the proximity of the crystals to suppress the probability of a partial energy deposition [49]. High energy gamma and electron events from sources located in the proximity of the crystals (or in the crystals themselves) are expected to be another major contribution to the background once alphas and muons have been removed. High-resolution experiments that are not based on thermal detectors for the search for double beta decay, like the LEGEND program, are facing a similar challenge and moving towards a similar solution [50, 51], although easier to implement as, in that case, the mounting structure doesn't play any thermal role nor needs to operate at mK temperature. The active assembly appears to be a major strategic advantage, as it tackles the problem of gamma and beta backgrounds with a general approach whose effectiveness doesn't depend on the choice of a particular isotope or the presence of a particular gamma line.

The possible applications of the active structure technique in the evolutionary framework of thermal detector experiments are summarised in Fig. 2, where green arrows indicates evolution steps where adding scintillating plastic to the previous generation setup is sufficient to hit the target background, while red arrows are steps where it is required but should be coupled to other technological improvements. Inside each arrow, some other relevant features of the experiment where the technique is applied are reported, namely the fact that some level of particle identification is already implemented, or the fact that double beta decay Q-value is below (low) or above (high) the 2615 keV gamma line from natural radioactivity.

3 Detectors construction and operation

In this section we summarize a phased approach to demonstrating the possibility of operating thermal detectors assembled in a structure made of plastic material. This is a mandatory preparatory step towards the full technological development of active scintillating structures, as large thermal detectors have always been operated inside copper structures. After building and operating a small size proof-of-principle detector, we switched to kilogram-scale state of the art detectors with two orders of magnitude larger sensitive volume and heat capacitance without observing any objective limitation in their performance compared to classical assembly methods.

3.1 Small scale proof-of-principle

The possibility of operating cryogenic single-particle detectors mounted in an acrylic mechanical structure has been successfully demonstrated in [52]. Tellurium dioxide crystals of $1 \times 1 \times 1$ cm^3 have been operated at a base temperature of $\sim$ 20 mK for extended

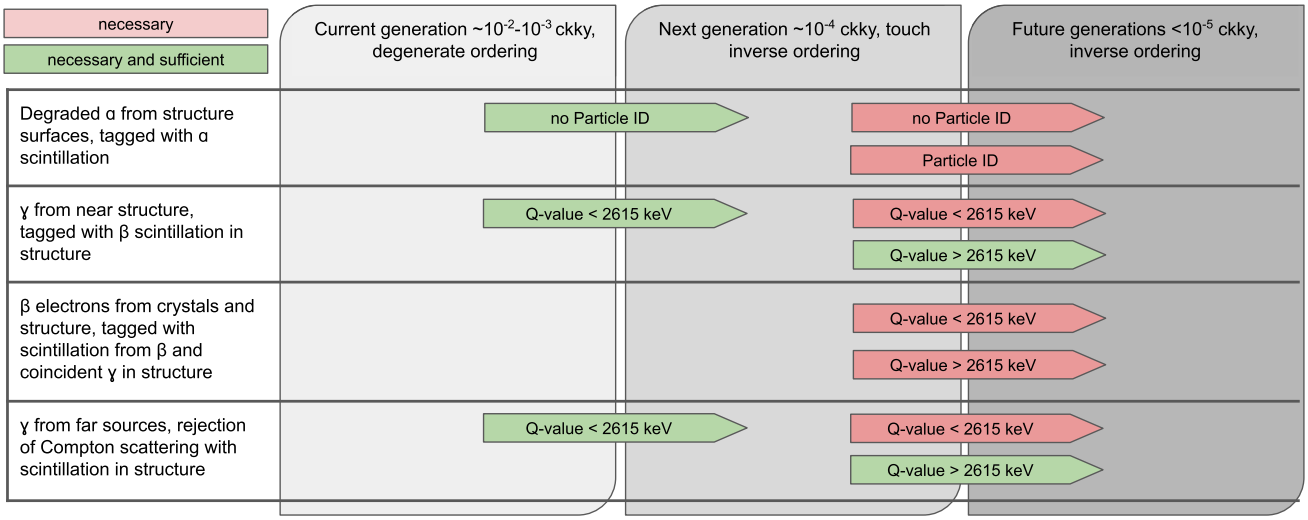

Fig. 2 The main (measured and expected) contributions to the background of double beta decay experiments based on cryogenic detectors are reported on the left. The columns report the background target of each generation in counts/(keV × kg × yr) and the corresponding physics reach in terms of neutrino mass ordering that can be explored/excluded. The arrows represent the fact that the technique described in this paper has the ability to reduce a given contribution to the level required to move from one generation to the following. Inside each arrow, some other relevant features of the experiment where the technique is applied are reported, namely the fact that the experiment already implements some level of particle identification (e.g. via dual heat-light readout or pulse shape discrimination) or the fact that the double beta decay Q-value is below or above the 2615 keV gamma line from natural radioactivity

periods of time with excellent stability. The performance of the detectors has been assessed both in terms of energy resolution (compatible with that of an equivalent detector assembled in a classical copper structure) and pulse shape. The pulses collected from the detectors in the plastic structure are generally faster (the rise time of the pulse is shorter) then those from the copper structure for the same thermal bath temperature. This is due to the fact that, due to the relatively large amount of loosely thermalised plastic material enclosing the absorber, the detector itself operates at a slightly higher temperature. From the mechanical point of view no detectable damage is reported due to the thermal cycle.

3.2 Full size single module demonstrator

A larger detector assembled with the same technique as the one described in the previous section has been built and operated in order to study how the detector performance scales with the size of the absorber. A two-floors tower has been assembled with $5 \times 5 \times 5$ cm^3 tellurium dioxide (TeO_2) crystals. This is the typical absorber used by the CUORE experiment for the search for neutrino-less double beta decay, and amongst the largest crystals ever used for this kind of application. The detector was installed in a dilution refrigerator in the Hall A at Laboratori Nazionali del Gran Sasso (LNGS), the former MIBETA [53], CUORICINO [54], CUORE-0 [24] and CUPID-0 [11] cryostat. Each TeO_2 crystal was instrumented with two Neutron Transmutation Doping thermistors (NTDs) for the read-out of the temperature signal and a silicon resistor (heater) [55] to inject controlled heat pulses for thermal gain stabilisation purposes. This setup is the same commonly used by the CUORE and CUPID experiments family and related R &Ds, as thoroughly described for example in [56]. Both NTDs and heaters where gold-wire bonded to a twisted constantan readout wiring glued to the mechanical structure and routing the signals to and from the thermalizations at the mixing chamber level. From the mixing chamber the signal was further routed outside the cryostat where the front-end electronics and digitization system is located. With the detectors operated between 10 and 20 mK, a suitable working point has been chosen in such a way that the working resistance of the NTDs was between 5 and 12 MΩ. The corresponding sensitivities, evaluated at the 2615 keV calibration line, was between 100 and 250 μV/MeV (for comparison, CUORE detectors are reported to operate with sensitivities in the 100–400 μV/MeV range [57] during normal operation). The acquired signals have been analysed with the typical analysis procedure adopted for thermal detectors, as described, again, in [56]. The mechanical structure of the detector is clearly visible in Fig. 3. A single piece of acrylic (Stratays Veroclear® [58]) has been built with additive manufacturing technique and cured with UV-light. The four vertical columns (with a roughly circular cross section about 5 mm in diameter) support a squared base 5 mm thick where the two crystals, separated by a 0.5 mm crossed-shape spacer, sit held by gravity (the idea of "gravity assisted" assembly is already proven [22] alternative to the classical approach where each crystal is independently constrained within a structure that removes all degrees of freedom [24]). At the top of each column a threaded hole allows the connection of the plastic structure to the copper cold plate (acting as the main thermal anchoring point for the whole detector as it is strongly linked to the mixing chamber). The topmost crystal is separated from the plate by an extra spacer.

An important parameter to assess the feasibility of this kind of assembly is the thermalization of the detectors, i.e. the rate at which the heat flows from the sensitive elements to the thermal bath. As shown in Fig. 4, the cooling rate of the TeO_2 detectors is

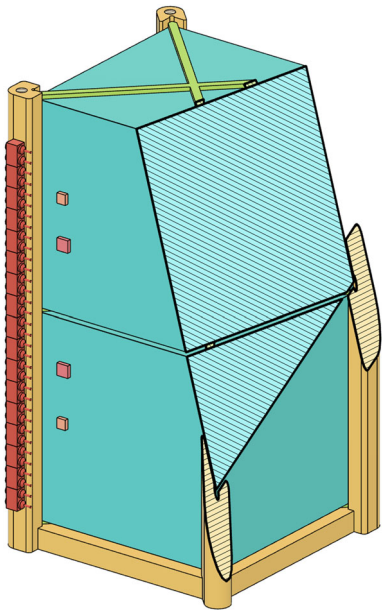

Fig. 3 A picture of the acrylic assembly containing the two $5 \times 5 \times 5$ cm^3 TeO_2 crystals attached to the copper cold plate in the Hall A dilution refrigerator at LNGS. On the side of the detector there are four smaller detectors with copper structures (data from these detectors are not used in this work). In the same run, a larger traditional copper structure with four $4.5 \times 4.5 \times 4.5$ cm^3 Li_2 MoO_4 crystals was attached below the acrylic setup and used as a benchmark for thermalization and performance. In the inset a sketch with the basic elements of the setup from the CAD design (yellow: acrylic structure, cyan: crystals, red: wring connectors, orange: NTDs and heaters

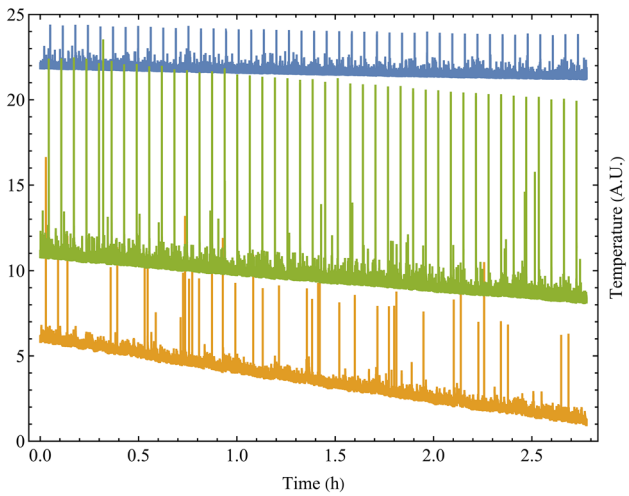

Fig. 4 Comparison between the evolutions of the baseline level (proxy for the detector temperature) of the TeO_2 detectors (orange and green) and one Li_2 MoO_4 (blue, for reference) during a ∼3 h period after partial warm-up. The cooling rate is comparable or faster for the acrylic structure. The periodic spikes are heater pulses (heater was not functional on one of the two TeO_2 detectors during this run)

similar or even faster compared to that of a lithium molibdate crystal, despite the latter being assembled in a more classical copper structure (identical to the one described in [22]). This confirm that also in this case, as already stated in [52, 59], the main thermal link between the detectors and the thermal bath is not the structure but the read-out wiring. Moreover, any thermal load that could be generated by heat release mechanisms at cryogenic temperatures, which are typical of amorphous compounds on the time scale of tens of hours [60], is negligible if present.

Figure 5 shows a typical pulse generated by a 2615 keV gamma interaction read out by the NTD thermistor. Also in this case no unexpected features are highlighted, and the pulse show a time evolution compatible with that of a similar detector operated in a classical copper structure. Rise time for the pulses is ∼20 ms at the working point, while decay time is ∼500 ms allowing the waveform to return to the baseline level within the 5 s acquisition window.

A ∼3 days campaign of calibration with high activity ^{232}Th source (resulting in ∼ 200 mHz counting rate on the detectors) resulted in the energy spectrum reported in Fig. 6.

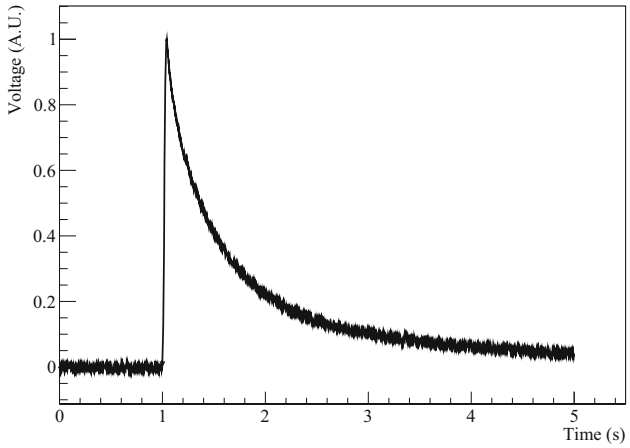

Fig. 5 Typical pulse recorded by a TeO_2 detector for a 2615 keV energy deposition. Despite being assembled in a highly insulating structure, the time constants are within the normal operating range and are fully compatible with the standard event reconstruction algorithms. No unexpected time constants or slow thermalization effects are observed, confirming the results of [52] with larger detectors

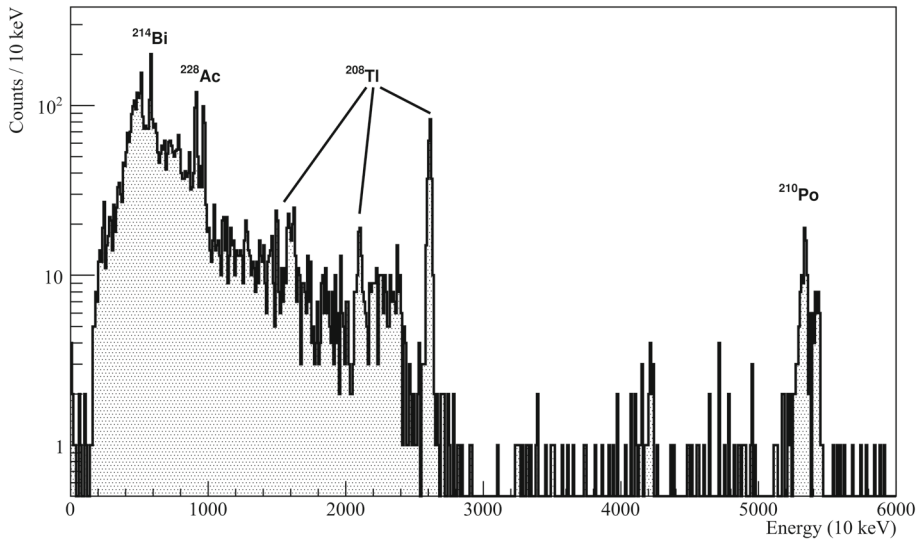

Fig. 6 Energy spectrum acquired with $5 \times 5 \times 5$ cm^3 TeO_2 detectors assembled in the acrylic structure. The statistics corresponds to about 3 days of data taking with high rate ^{232}Th calibration sources. The 2615 keV gamma line from ^{208}Tl is clearly visible and used to estimate the energy resolution of 10–20 keV FWHM depending on the considered channel and working point. Other gamma lines from the calibration source are clearly visible, as well as the prominent alpha lines from ^{210}Po internal and external contaminations, common in these types of measurements, demonstrating the normal operation and good performance of the detectors

With an energy resolution between 10 and 20 keV FWHM at the 2615 keV ^{208}Tl line, achieved without extensive noise or working point optimization, the performance of the detectors assembled in the acrylic structure is considered very promising and in line with that of other thermal detectors used for double beta decay searches [11]. Thanks to the achieved energy resolution, all the expected spectral features across the typical dynamic range are clearly visible despite the limited statistics.

Despite the normal operation during the periods at base temperature, after two thermal cycles (room temperature to 10 mK and back to room temperature) the acrylic structure showed some level of damage due to mechanical stresses following differential thermal contractions between the columns and the contained crystals. A careful reanalysis of the setup and dedicated finite element simulations showed that not enough vertical play between the upper face of the top crystal and the copper plate was included in the design to account for the columns shortening. This issue, although easily addressable with a more careful engineering process, highlighted a technical criticality of this specific design that is discussed in the next section.

Fig. 7 Design of monolithic structure, manufactured as a single unit. Crystals are stacked inside the structure separated by thin spacers. As the structure shortens during cool-down the dimensional tolerances are a critical aspect of the engineering process. The collection of the scintillation light is facilitated by the uninterrupted design of the vertical columns and light sensors can be places either at the top of the tower, or even remotely and the photons collected and transported by means of optical fibres

4 Design alternatives and technical outlook

As described in the previous section, a monolithic structure with vertical columns running along the entire tower length (Fig. 7) can be realized. This design has some relevant advantages: the reduced number of elements in the detector setup simplifies the cleaning and assembly procedures: the detectors (both crystals and light-sensitive devices) are simply slid into place and later instrumented with thermistors and heaters and bonded to wiring strips glued to the columns. Moreover, the light signal produced by scintillation of the structure is naturally guided along the columns towards the top and bottom of the tower, where it can be collected directly by a light sensitive element or further routed to a warmer stage of the system through optical fibres optically coupled to the acrylic material or directly embedded into it. At the same time, the monolithic nature of this design poses a challenge in the evaluation of the effects of thermal contractions: the long vertical columns shortens noticeably during cool-down, resulting in an increase in the compression load on the crystals. If dimensional tolerances are not properly included in the design and engineering phase, the resulting stresses can lead to mechanical failures of the acrylic structure or of the contained sensitive elements (crystal and/or light detectors), as described in Sect. 3.2. The implementation of this kind of structural design therefore requires a complete study and deep understanding of the mechanical properties of the material at the different temperatures and of it's behaviour during the cool down cycle.

Figure 8 shows an alternative approach to the design of the detector structure that further reduces the amount of material. The vertical columns of Fig. 7 are replaced by four cables that support the weight of the detectors. The acrylic structures, in this case, serve only the purpose of spacers between crystals and light detectors, as well as an anchoring point for the wiring strips (not shown in the figure). Since they don't support any structural load, they can be very thin and light structures, further reducing their potential impact as background sources in the experiment. Optical continuity is not granted in this case, therefore, in situ low temperature light detectors are required to detect light produced by the acrylic frames (if scintillation is implemented).

The material for the supporting cables can be either acrylic itself (in this case the fibre can be made of the same scintillating or non-scintillating plastic of the frames) or a more structurally sound material, like Poly-paraphenylene terephthalamide (Kevlar®), whose application as structural material in cryogenic applications is exceptionally well proven by the CUORE experiment [61, 62].

5 Conclusions

We described an alternative approach to the construction of supporting structures for single-particle cryogenic detectors. The recent results obtained with two full-size CUORE-like detectors assembled in an acrylic structure and successfully operated in a cryostat at LNGS are reported, showing that single-particle, kilogram scale thermal detectors can be operated with non-conductive assemblies. By replacing the typically used passive material (copper) in the vicinity of the sensitive elements of the detector with lower-Z, lower-density acrylic structures, a beneficial reduction of the background should be achieved by reducing the probability that radiation

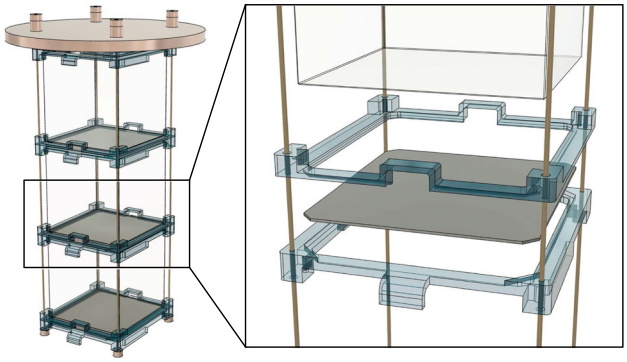

Fig. 8 Design of a cable-based structure. As the weight of the detectors is supported by the cables only, the other structures can be reduced to a very minimal design as they only serve the purpose of spacers between crystals and light detectors. All the element are simply stacked and dimensional tolerances are relaxed as the overall length of the tower, as well as the compression load due to thermal contractions, can easily be adjusted by changing the tension of the cables or by means of an elastic element at the interface with the cryostat. In this case there is no continuity of the optical elements, therefore light (if scintillation needs to be implemented) must be read at each floor by an independent light sensitive device

loses energy in a passive element of the setup thus polluting the ROI of the experiments. A further reduction of the background achievable by making this material a scintillator, and therefore an active element, can be expected [49].

Acknowledgements We thank Marco Iannone from INFN - Section of Roma1 and member of the Hammer project for helping with the production and preparation of the 3D printed components of the assembly. We recognise the contribution of LNGS staff for the operation and maintenance of the experimental facility where the measurements were taken.

Funding Open access funding provided by Università degli Studi di Milano - Bicocca within the CRUI-CARE Agreement.

Data Availability Statement This manuscript has associated data in a data repository. [Authors' comment: Data will be made public under explicit request.]

Code availability The software will be made public under explicit request.

Declarations

Conflict of interest The authors have no financial or proprietary interests in any material discussed in this article.

References

1. P.A. Zyla et al. (Particle Data Group), Progress of Theoretical and Experimental Physics 2020, **083C01** (2020)
2. C. Adams et al., arXiv:2212.11099
3. D.Q. Adams et al., Phys. Rev. Lett. **126**(17), 171801 (2021). https://doi.org/10.1103/PhysRevLett.126.171801
4. O. Azzolini et al., Phys. Rev. Lett. **123**(26), 262501 (2019). https://doi.org/10.1103/PhysRevLett.123.262501
5. E. Armengaud et al., Eur. Phys. J. C **80**, 674 (2022). https://doi.org/10.1140/epjc/s10052-020-8203-4
6. M. Agostini et al., J. Phys. G **40**(3), 035110 (2013). https://doi.org/10.1088/0954-3899/40/3/035110
7. N. Ackerman et al., Phys. Rev. Lett. **107**(21), 212501 (2011). https://doi.org/10.1103/PhysRevLett.107.212501
8. A. Gando et al., Phys. Rev. C **85**(4), 045504 (2012). https://doi.org/10.1103/PhysRevC.85.045504
9. M.J. Dolinski, A.W.P. Poon, W. Rodejohann, Neutrino-less double-beta decay: status and prospects. Ann. Rev. Nuclear Part. Sci. **69**(1), 219–251 (2019)
10. D.Q. Adams et al., Nature **604**(7904), 53 (2022)
11. L. Cardani et al., J. Low Temp. Phys. **199**, 425–432 (2020). https://doi.org/10.1007/s10909-020-02382-w
12. E. Armengaud et al., Phys. Rev. Lett. **126**, 181802 (2021)
13. H.B. Kim et al., J. Low Temp. Phys. **209**, 962–970 (2022)
14. D'Andrea et al., Universe **7**(9), 341 (2021). https://doi.org/10.3390/universe7090341
15. S. Abe et al., Phys. Rev. Lett. **130**, 051801 (2023). https://doi.org/10.1103/PhysRevLett.130.051801
16. S. Al Kharusi et al., Phys. Rev. D **104**(11), 112002 (2022). https://doi.org/10.1103/PhysRevD.104.112002
17. J. Caravaca et al., (SNO Collaboration), Int. J. Mod. Phys. A **35**(34–35), 2044013 (2020). https://doi.org/10.1142/S0217751X20440133
18. S. Verma et al., Nuclear Instrum. Methods Phys. Res. A **1046**, 167634 (2023)
19. S. Pirro, P. Mauskopf, Ann. Rev. Nuclear Part. Sci. **67**, 161–181 (2017)
20. Yong-Hamb. Kim et al., Superconduct. Sci. Technol. **35**, 063001 (2022)

21. R. Artusa et al., Eur. Phys. J. C **74**, 2956 (2014)
22. K. Alfonso et al., Eur. Phys. J. C **82**, 810 (2022)
23. D.Q. Adams et al., Progr. Part. Nuclear Phys. **122**, 103902 (2022)
24. C. Alduino et al., J. Instrum. **11**, P07009 (2016). https://doi.org/10.1088/1748-0221/11/07/P07009
25. E. Armengaud et al., Eur. Phys. J. C **80**(1), 44 (2020). https://doi.org/10.1140/epjc/s10052-019-7578-6
26. O. Azzolini et al., Phys. Rev. Lett. **129**, 11 (2022). https://doi.org/10.1103/PhysRevLett.129.111801
27. CUPID Interest Group, arXiv:1907.09376
28. A. Luqman et al., Nuclear Instrum. Methods Phys. Res. A **855**, 140–147 (2017). https://doi.org/10.1016/j.nima.2017.01.070
29. O. Azzolini et al., Eur. Phys. J. C **79**(7), 583 (2019). https://doi.org/10.1140/epjc/s10052-019-7078-8
30. C. Alduino et al., Eur. Phys. J. C **77**, 543 (2017)
31. V. Alenkov et al., Eur. Phys. J. C **82**, 1140 (2022)
32. The SNO Collaboration, Nuclear Instrum. Methods Phys. Res. A **449**, 172–207 (2000)
33. V.N. Salimgareeva, S.V. Kolesov, Instrum. Exp. Tech. **48**, 273–282 (2005)
34. D.G. Kim et al., Nuclear Eng. Technol. **52**(12), 2910–2917 (2020)
35. M. Biassoni et al., Eur. Phys. J. C **75**, 480 (2015)
36. V. Novati et al., Nuclear Instrum. Methods Phys. Res. A **940**, 320–327 (2019). https://doi.org/10.1016/j.nima.2019.06.044
37. V. Singh et al., arXiv:2210.15619
38. A. Erhart et al., arXiv:2205.01718
39. M. Biassoni, O. Cremonesi, Progr. Part. Nuclear Phys. (2020). https://doi.org/10.1016/j.ppnp.2020.103803
40. A. Armatol et al., Toward CUPID-1T. arXiv:2203.08386
41. M. Agostini et al., arXiv:2202.01787
42. V. Alenkov et al., arXiv:1512.05957
43. A. Giuliani et al., Eur. Phys. J. C **78**, 272 (2018)
44. M. Agostini et al., J. High Energy Phys. **2023**, 172 (2023). https://doi.org/10.1007/JHEP02(2023)172
45. I. Dafinei et al., Nuclear Instrum. Methods Phys. Res. A **554**(1–3), 195–200 (2005). https://doi.org/10.1016/j.nima.2005.08.010
46. L. Canonica et al., Nuclear Instrum. Methods Phys. Res. A **732**, 286–289 (2013). https://doi.org/10.1016/j.nima.2013.05.114
47. R. Strauss et al., Eur. Phys. J. C **75**, 352 (2015)
48. A. Armatol et al., Phys. Rev. C **104**, 015501 (2021). https://doi.org/10.1103/PhysRevC.104.015501
49. S. Ghislandi et al., Il Nuovo Cimento C **44**(2–3), 1–4 (2021). https://doi.org/10.1393/ncc/i2021-21093-6
50. L. Manzanillas et al., J. Instrum. **17**(3), C03031 (2022). https://doi.org/10.1088/1748-0221/17/03/C03031
51. L. Manzanillas et al., J. Instrum. **17**(9), P09007 (2022). https://doi.org/10.1088/1748-0221/17/09/P09007
52. M. Biassoni et al., Eur. Phys. J. Plus **136**, 986 (2021). https://doi.org/10.1140/epjp/s13360-021-01978-9
53. S. Pirro et al., Nucl. Inst. Methods Phys. Res. A **444**, 71–76 (2001)
54. E. Andreotti et al., Astropart. Phys. **34**(11), 822–831 (2011)
55. E. Andreotti et al., Nuclear Instrum. Methods A **664**, 161 (2012)
56. C. Alduino et al., Phys. Rev. C **93**(4), 045503 (2016). https://doi.org/10.1103/PhysRevC.93.045503
57. K. Alfonso et al., Nucl. Inst. Methods Phys. Res. A **1008**, 165451 (2021). https://doi.org/10.1016/j.nima.2021.165451
58. https://www.stratasys.com/-/media/files/material-spec-sheets/mds_pj_veroclear_0320a.pdf
59. M. Biassoni et al., J. Low Temp. Phys. **206**(1–2), 80–96 (2022). https://doi.org/10.1007/s10909-021-02639-y
60. F. Pobell, *Matter and Methods at Low Temperatures* (Springer, Berlin, 2007)
61. C. Alduino et al., Cryogenics **102**, 9–21 (2019)
62. A. Bersani et al., Cryogenics **54**, 50 (2013)